Atomic Scale Imaging: A Hands-On Scanning Probe Microscopy Laboratory for Undergraduates

Chuan-Jian Zhong,* Li Han, Mathew M. Maye, Jin Luo, Nancy N. Kariuki, and Wayne E. Jones, Jr.
Department of Chemistry and Institute of Materials Research, State University of New York, Binghamton, NY 13902;
cjzhong@binghamton.edu

Many students have traditionally had difficulty learning atomic and molecular scale concepts in chemistry. The reason for this is not certain, but challenges associated with visualizing atoms and molecules are thought to be at the core of the issue *(1)*. A variety of computer simulation and chemical modeling approaches have provided some means for learning enhancement *(2)*. Educational studies have suggested that hands-on experiences provide students an improved opportunity for understanding abstract atomic and molecular level concepts. With the plethora of advanced microscopic techniques available, the key to improved understanding of atoms and molecules could be to put these tools in the hands of our undergraduate learners.

Microscopic techniques such as optical microscopy, scanning electron microscopy, and transmission electron microscopy (TEM) have been used in undergraduate laboratories for a few years. With the exception of high-resolution TEM, these technologies cannot provide atomic resolution. Scanning probe microscopy (SPM) is a collective term referring to a family of powerful surface imaging techniques, among which scanning tunneling microscopy (STM) and atomic force microscopy (AFM) are the basic techniques *(3)*. The capability of STM and AFM to use completely different physical principles to visualize materials at atomic scales provides an advanced solution to the above problem. A few recent reports have demonstrated the importance of introducing STM *(4–10)* and AFM *(11)* into the undergraduate laboratories. There is, however, a critical gap between experiments and learning activities at an atomic scale *(5–6)*. Part of the gap is due to the requirement of conductive samples for STM *(12)*, limiting the scope of inquiry-based learning. In view of the applicability of AFM to almost any sample, the combination of STM and AFM serves as an effective means for enhancing the learning process.

Why would we want our students to visualize atoms in the laboratory? The existence of atoms or molecules in materials is an important chemical concept. Students usually have difficulty with perception of the size and number of atoms present within a given substance. Optical microscopes can examine objects in fine detail, but cannot visualize things as small as atoms due to the limitation that only objects larger than the wavelength of the light can be resolved. Secondly, the arrangement of atoms at the nanometer scale determines macroscopic properties of a material. Students usually have difficulty in correlating the atomic-scale structure with the macroscopic properties for materials of similar elemental composition. For example, diamond and graphite are composed exclusively of carbon atoms. Their atomic arrangements are very different however. In diamond, each carbon atom is bonded to four others to form a strong network. In graphite, each carbon atom is bonded to three others and arranged in sheets with weak intersheet interactions. Diamond is transparent and hard, whereas graphite is black and soft.

We describe herein one of a series of combination STM–AFM laboratory exercises that is aimed at enhancing the comprehension of atomic and molecular scale concepts and providing hands-on experience to help undergraduate students understand the basic theory and operation of SPM. This understanding includes how STM functions through electron tunneling, how AFM functions through interatomic interaction, and how SPM supports atomic theory through atomic-scale imaging of well-defined crystalline materials, such as highly ordered pyrolytic graphite (HOPG) *(13–14)* and muscovite mica, $KAl_3Si_3O_{10}(OH)_2$ *(14–15)*. The experiments were tested in both Instrumental Methods of Analysis and Introductory Analytical Chemistry laboratories at SUNY-Binghamton.

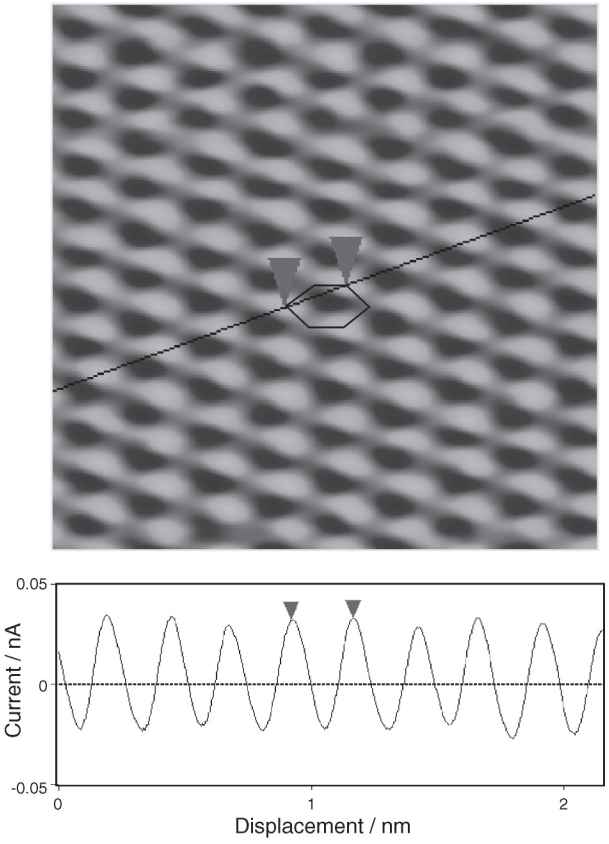

Figure 1. STM image of highly ordered pyrolytic graphite (HOPG, 2-nm × 2-nm, 8 Hz). The cross-section view below the image corresponds to the line drawn in the image.

Results

STM Images of HOPG

The typical STM image of HOPG, shown in Figure 1, exhibits a hexagonal pattern of bright spots whose nearest-neighbor distance is about 0.25 nm. As explained below and indicated by the drawing of a hexagonal ring in the figure, these spots are from alternate carbon atoms in the surface layer of the graphite structure. The atomic periodicity and apparent interatomic distances are shown in the cross-section view.

A higher resolution image obtained at a lower scan rate (Figure 2) exhibits a honeycomb hexagonal pattern that includes all of the carbon atoms in the surface layer. Each hexagon consists of three brighter spots separated by three fainter spots, as indicated by the intensity differences in the cross-sectional view. The spacing between the two nearest bright spots is 0.25 nm, whereas the distance between nearest-neighbor (brighter-fainter) spots is 0.14 nm.

AFM Image of Mica

Figure 3 shows a typical contact-mode AFM image of a muscovite mica sample. A hexagonal array of bright spots, or body-centered hexagonal array, is evident. As displayed by the cross-section view, the distance between the two nearest-neighboring brighter spots is about 0.52 nm.

Discussion

Interpretation of the STM Image of HOPG

To understand the imaging results in comparison with the expected crystalline structures, we focus first on the discussion of the dependence of tunneling current on electron density. Because of differences in the relative position of atoms to their neighboring layer, there exists a nonequivalency of atoms (A and B) in any single layer *(3a, 13)*. For HOPG, the fact that a freshly-cleaved layer can be exposed by pressing and pulling off with clear tape helps students understand the layered structure of HOPG. The electrons around the Fermi level are mainly in p_π orbitals. The type-A carbon atoms have neighbors directly below in the second layer, whereas the type-B atoms are located above the empty centers of the hexagons of the layer beneath. Atom B has a higher electron density than that of atom A due to differences in the local density of states at the surface by interlayer interactions. The favorable overlap of p_π orbitals on the A sites stabilizes the electron energy relative to the Fermi level (Figure 4a). In contrast, the absence of overlap for B sites leaves the electron energy near the Fermi level. The electron-rich B sites thus have a larger tunneling current than on the A sites and appear as the bright spots in the image. The "3-for-hexagon" pattern can be assigned to B atoms (Figure 4b). The center to center atomic distance in this image is 0.25 nm, which is

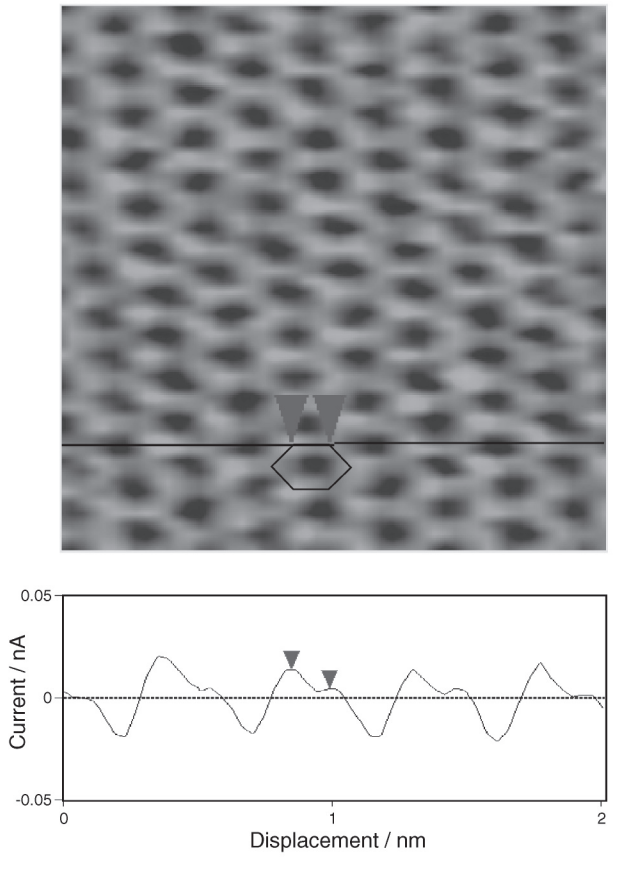

Figure 2. STM image of highly ordered pyrolytic graphite (HOPG, 2-nm × 2-nm, 8 Hz). The cross-section view below the image corresponds to the line drawn in the image.

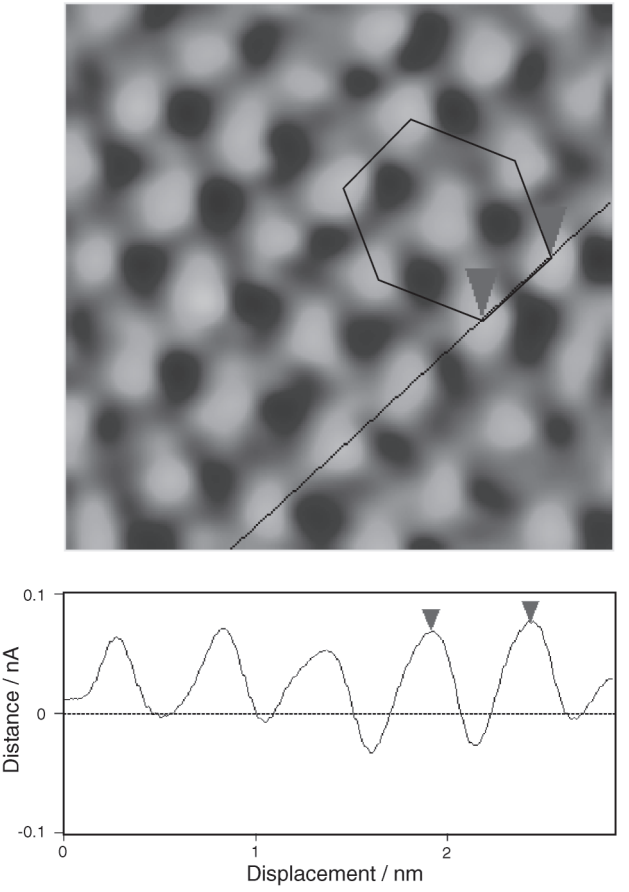

Figure 3. AFM image of muscovite mica (3-nm × 3-nm). The cross-section view below the image corresponds to the line drawn in the image.

consistent with the next nearest-neighbor distance (0.246 nm) for HOPG. The nearest-neighboring atomic distance (brighter-to-fainter, 0.14 nm) and the next nearest-neighbor distance (brighter-to-brighter, 0.25 nm) leads to a hexagonal closed-packed pattern of rings, that is "6-for-hexagon". The brighter and the fainter sites, though not fully resolved, can be assigned to B and A sites, respectively (Figure 4c). The A–A or B–B (0.25 nm) and A–B (0.14 nm) distances are consistent with the crystalline structure.

A second possible explanation is mechanical, based on how hard it is to depress the atoms in HOPG (i.e., on local mechanical hardness). The B-site is depressed less than the A-site by the tip force, that is the B-site is harder than the A-site. This difference is based on an atom–atom potential calculation of the tip-sample repulsive interaction *(16–18).* The atom-site with greater repulsive force (B) resists the compression effect of the tip force more greatly. The mechanical explanation seems reasonable because variations do exist in the local mechanical hardness between A, B, and hollow sites. The positions of the atoms seen in AFM images correspond to the positions of the atoms of the B-type in STM images. Further consideration of both electronic and mechanical effects based on current literature of AFM, STM, and molecular orbital calculations of HOPG could serve as starting points of inquiry-based learning for students to explore issues related to the atomic scale visualization *(3, 16–18).*

Interpretation of the AFM Image of Mica

The structure of muscovite mica is complex, but its cleavage planes lie between two layers of SiO_4^{4-} tetrahedra that sandwich a layer of potassium ions, K^+ (some tetrahedra contain Al atoms instead of Si atoms). The tetrahedra share corners in such a way that the oxygen atoms have a nearest-neighbor distance of 0.28 nm and form six-membered rings around the potassium ions, which have a nearest-neighbor distance of 0.52 nm. There are two possible explanations for the hexagonal pattern observed in Figure 3. The first is that the K^+ ions are removed when cleavage takes place. The dark spots are holes where the K^+ ions were and the bright spots are unresolved oxygen atoms. A second explanation is that the brighter spots are K^+ ions that are still present in the hexagonal holes between the oxygen rings. In both cases the pattern would be hexagonal and the repeat distance would be what is observed, 0.52 nm. A difficulty with both explanations is that it seems unlikely that all of the K^+ ions would be left on one side of the cleaved plane *(19–22).* Figure 5 illustrates the two possible surface patterns that would result. A detailed understanding of the atoms visualized is an open-ended question because there exist ambiguities about the fate of K^+ ions based on model simulations *(20–22).*

Hazards

The chemicals involved in this experiment pose no significant hazards.

Summary

In summary, we have developed a new hands-on laboratory experiment utilizing both STM and AFM in the undergraduate laboratory. The experiment emphasizes atomic scale visualization of well-defined crystalline materials. A number of open-ended questions can be generated when interpreting the image results in terms of atomic-scale effects on tunneling current and tip-sample interaction. The students benefit from the experiment in grasping atomic scale concepts and participating in further inquiry-based learning activities. In view of the simplicity of sample preparation and the increased availability of SPM instrumentation, we encourage others to consider incorporating this experiment into their undergraduate chemistry curriculum.

Supplemental Material

Additional background material, the experimental procedure, and notes for data processing are available in this issue of *JCE Online*.

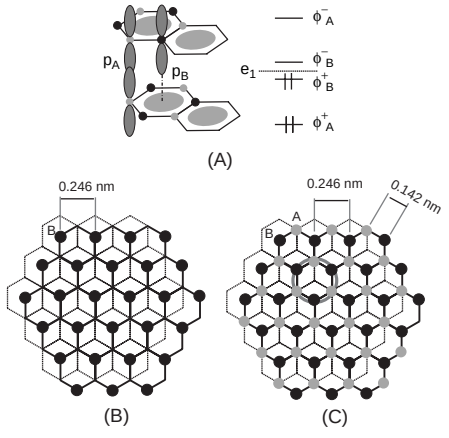

Figure 4. Schematic illustration of two types of atomic arrangements that are detected by STM on the surface of highly ordered pyrolytic graphite. (A) p_π orbital interactions between ϕ_A and ϕ_B, and the band orbitals (e_f: Femi level). (B) 3-for-hexagon pattern. (C) 6-for-hexagon pattern.

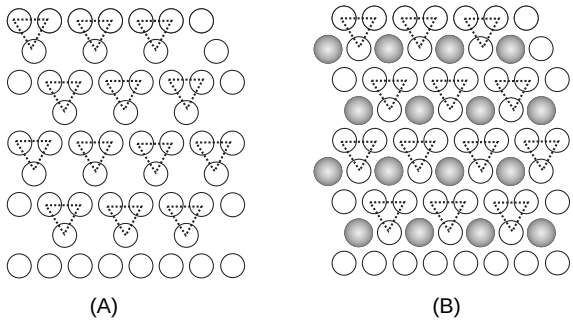

Figure 5. Schematic illustration of two types of atomic arrangements that are detected by STM for a mica surface. The triangles represent groups of three O atoms that would be unresolved by AFM. (A) O atoms, and (B) O and K atoms. Open circles: O atoms. Filled circles: K atoms.

Acknowledgments

Financial support of this work is gratefully acknowledged from the National Science Foundation CCLI program (EDU-9952628), ACS–PRF, 3M, and the NSF Division of Materials research (DMR 9976713). We appreciate helpful discussions with V. Jones, J. Kenseth, and S. Wong.

Literature Cited

1. (a) Susan Montgomery in "Addressing Diverse Learning Styles Through the Use of Multimedia" *http://fie.engrng.pitt.edu/fie95/3a2/3a22/3a22.htm* (accessed Oct 2002). (b) Felder, R. M. *J. College Science Teaching* **1993,** *23*(5), 286–290. (c) Wright, J. C. *J. Chem. Educ.* **1996,** *73,* 827. (d) Bodner, G. M. *J. Chem. Educ.* **1986,** *63,* 873. (e) Penick, J. E. *The Science Teacher* **1994,** *61,* 30–33. (f) Shiland, T. W. *J. Chem. Educ.* **1999,** *76,* 107 and references therein.
2. (a) Rioux, F. *Chem. Educator* **1999,** *4* (2), 40. (b) Lyon, J. M. *Chem. Educator* **1998,** *3* (6), S1430. (c) Shusterman, A. J.; Hoistad, L. M. *Chem. Educator* **2001,** *6* (1), 36.
3. (a) Magonov, S. N.; Whangbo, M. H. Eds. *Surface Analysis with STM and AFM;* VCH Publishers: Weinhelm, 1996. (b) Bonnell, D. A., Ed. *Scanning Tunneling Microscopy and Spectroscopy. Theory, Techniques, and Applications:* VCH Publishers: Weinhelm, 1993. (c) Takano, H.; Kenseth, J. R.; Wong, S. -S.; O'Brien, J. C.; Porter, M. D.; *Chem. Rev.* **1999,** *99,* 2845. (d) For a detailed description of STM and AFM, see the Web site at *http://matlabs.clt.binghamton.edu/spm/matspmindex.htm* (accessed Oct 2002).
4. Braun, R. D. *J. Chem. Educ.* **1992,** *69,* A90.
5. Rapp, C. S. *J. Chem. Educ.* **1997,** *74,* 1087.
6. Glaunsinger, W. S.; Ramakrishna, B. L.; Garcia, A. A.; Pizziconi, V. *J. Chem. Educ.* **1997,** *74,* 310.
7. Poler, J. C. *J. Chem. Educ.* **2000,** *77,* 1198.
8. Giancarlo, L. C.; Fang, H. B.; Avila, L.; Fine, L. W.; Flynn, G. W. *J. Chem. Educ.* **2000,** *77,* 66.
9. Lorenz, J. K.; Olson, J. A.; Campbell, D. J.; Lisensky, G. C.; Ellis, A. B. *J. Chem. Educ.* **1997,** *74,* 1032A.
10. Skolnik, A. M.; Hughes, W. C.; Augustine, B. H. *Chem. Educator* **2000,** *5* (1), 8.
11. Coury, L. A., Jr.; Johnson, M.; Murphy, T. J. *J. Chem. Educ.* **1995,** *72,* 1088.
12. Binning, G.; Roher, H.; Gerber, C; Weibel, E. *Phys. Rev. Lett.* **1982,** *49,* 57.
13. Park, S. J.; Quate, C. F. *Appl. Phys. Lett.* **1986,** *48,* 112.
14. (a) Hartman, H.; Sposito, G.; Yang, A.; Manne. S.; Gould, S. A. C.; Hansma, P. K. *Clays and Clay Minerals* **1990,** *38,* 337. (b) see a detailed description of different micas, *http://www.unb.ca/courses/geol2142/LEC-26.html* (accessed Oct 2002).
15. Drake, B.; Prater, C. B.; Weisenhorn, A. L.; Gould, S. A. C.; Albrecht, T. R.; Quate, C. F.; Cannell, D. S.; Hansma, H. G.; Hansma, P. K. *Science* **1989,** *243,* 1586.
16. Atamny, F.; Spillecke, O.; Schloegl, R. *Phys. Chem. Chem. Phys.* **1999,** *1,* 4113.
17. Lee, K. H.; Causa, M.; Park, S. S. *J. Phys. Chem. B* **1998,** *102,* 6020.
18. Whangbo, M.-H.; Liang,W.; Ren, J.; Magonov, S. N.; Wawkuschewski, A. *J. Phys. Chem.* **1994,** *98,* 7602.
19. Ono, S. S.; Yao, H.; Matsuoka, O.; Kawabata, R.; Kitamura, N.; Yamamoto, S. *J. Phys. Chem. B* **1999,** *103,* 6909.
20. Tsujimichi, K.; Tamura, H.; Hirotani, A.; Kubo, M.; Komiyama, M.; Miyamoto, A. *J. Phys. Chem. B* **1997,** *101,* 4260–4264
21. Coleman, R. V.; Xue, Q.; Gong, Y.; Price, P. B. *Surf. Sci.* **1993,** *297,* 359.
22. Yoshida, I.; Sugita, T.; Sasaki, K.; Hori, H.; Kagaku, H. *J. Surf. Sci., Soc. Jpn.* **1996,** *17,* 90.